

Article

Impact of the Winding Arrangement on Efficiency of the Resistance Spot Welding Transformer

Gašper Habjan * and Martin Petrun 

Faculty of Electrical Engineering and Computer Science, University of Maribor, 2000 Maribor, Slovenia; martin.petrun@um.si

* Correspondence: gasper.habjan@um.si

Received: 31 July 2019; Accepted: 23 September 2019; Published: 30 September 2019



Abstract: In this paper, the impact of the winding arrangement on the efficiency of the resistance spot welding (RSW) transformer is presented. First, the design and operation of the transformer inside a high power RSW system are analyzed. Based on the presented analysis, the generation of imbalanced excitation of the magnetic core is presented, which leads to unfavorable leakage magnetic fluxes inside the transformer. Such fluxes are linked to the dynamic power loss components that significantly decrease the efficiency of the transformer. Based on the presented analysis, design guidelines to reduce the unwanted leakage fluxes are pointed out. The presented theoretical analysis is confirmed by measurements using a laboratory experimental system. The presented experimental results confirm that the proposed improved winding arrangement increased the efficiency of the transformer in average for 6.27%.

Keywords: DC-DC converter; resistance spot welding; transformer; efficiency; dynamic power loss; design

1. Introduction

Resistance spot welding (RSW) systems have a very important role in modern industry. Considering the automotive industry alone, their importance is striking, as nowadays three new cars are produced every second worldwide [1,2]. An interesting fact is that three to five thousand welding spots are required to produce a contemporary personal car. Such a high amount of welding spots requires, on the one hand, the use of fully automated welding systems that are based on robot arms and on the other hand consumes large quantities of energy. Therefore welding systems should be designed as high power density devices where the efficiency of the whole system is crucial.

RSW systems can be generally divided in two groups—systems that produce AC and systems that produce DC welding currents. Nowadays the DC RSW systems are generally replacing the older AC RSW systems due to several advantages [3,4]. A typical contemporary high power RSW system consists of a AC-DC converter that operates at a frequency around 1 kHz, which is generally classified as a medium frequency RSW system [4–7]. A medium frequency RSW system with a DC welding current is shown in Figure 1.

The first part of the discussed system is the AC-AC converter, which consists of a passive input rectifier, a DC-link and H-bridge inverter. The full-wave input rectifier produces a DC voltage U_{dc} from phase voltages u_a , u_b and u_c , whereas the H-bridge inverter generates a pulse-width modulated (PWM) voltage with modulation frequency of 1 kHz. The presented AC-AC converter supplies the primary side of a welding transformer and is in high power RSW system usually not mounted on a robot arm.

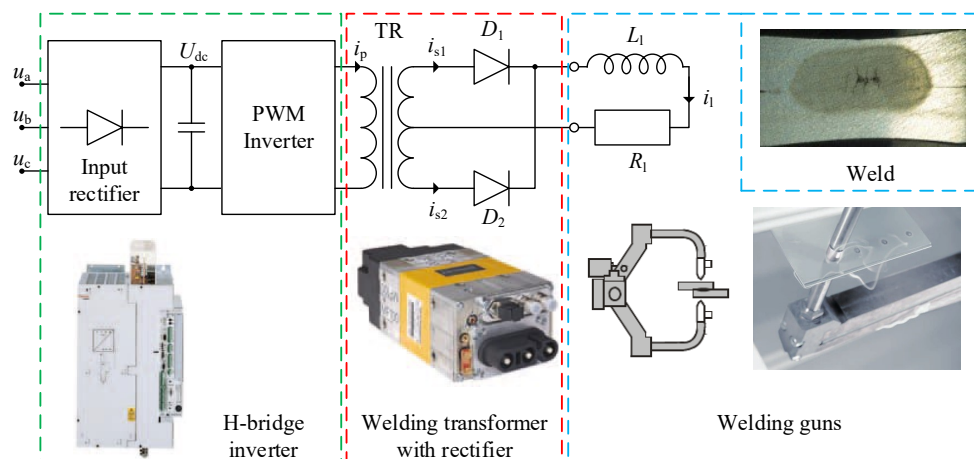


Figure 1. Schematic presentation of a typical resistance spot welding system [5].

The second part is a welding transformer, which consists of a three winding transformer with one primary and two secondary windings and an integrated center-tapped full-wave output rectifier. The main task of this transformer is to adequately increase the level of the primary current i_p , consequently a turn ratio of 55:1 is used. The high alternating currents i_{s1} and i_{s2} in both secondary windings are rectified to a DC welding current i_i using a center-tapped output rectifier where two special high current diodes are used.

The third part of the RSW system is a welding gun that is connected to the output rectifier. The main task of a welding gun is to produce weld of prescribed quality, for what adequate electrical, mechanical and thermal conditions have to be fulfilled [2,4]. Due to very high welding currents in such systems, the welding transformer and the welding gun have to be placed together as close as possible to reduce high ohmic power losses [3]. Consequently both discussed parts are mounted on a moving robot arm, whereas the high power density of the welding transformer is one of the main goals in its design process.

In the RSW systems, the majority of the power loss occurs in the second and third part of the system due to very high currents. Therefore these parts are generally cooled using a cooling liquid [3,6]. By reducing the generated power loss in these parts consequently less cooling is required and the power density of the devices can be increased. In this paper the main focus was to analyze the impact of the winding arrangement on the power loss of the welding transformer. For this purpose, a laboratory experimental system was assembled that enabled comparisons of different winding arrangements. The obtained results have shown that an adequate winding layout reduced the power loss in the welding transformer significantly. The main contribution of presented research work is that presented experimental results are supported by a sound theoretical background, where also guidelines for the designing of high power transformers with center-tapped output rectifiers are discussed. The presented theoretical background and design guidelines are indispensable in the design process of the device, as they give an adequate starting point and can be applied to any contemporary design method (e.g., applying adequate winding layout in an finite element model of the device, where the dimensions of the winding can be furthermore optimized).

The paper is organized as follows. In the first section an introduction for the discussed problem is given. In the second section operation and the power loss inside a RSW system are discussed. In the third section the laboratory experimental system is presented, whereas in the fourth section the obtained results are presented and discussed. The fifth section gives a conclusion, where also the outline for future work is presented.

2. Design, Operation and Power Loss Inside a RSW Transformer

Design, operation and power loss inside a RSW transformer are inseparably interconnected. Power loss inside the transformer depends both on the operation as well as the design of the transformer, where the main focus of this paper is reduction of power loss by improving the design of the transformer.

2.1. Design of the Welding Transformer

A typical welding transformer is assembled from an iron core on which three windings are placed as shown in Figure 2.

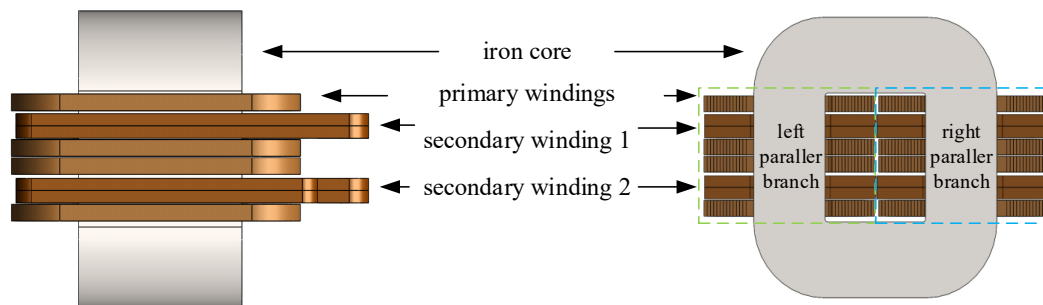


Figure 2. A typical design of a welding transformer [1].

The iron core consists of a wound sheet tape of a soft magnetic material that is wound on a model to obtain adequate geometry. The iron core is usually cut in two C-like segments to simplify the assembling process of the transformer [3,6,7]. The primary winding is generally obtained from a rectangular wire that is wound to adequate coils that fit on the iron core segments [3,7]. The primary winding is assembled using 4 such coils that are connected in series and have combined 55 winding turns. Due to high currents i_{s1} and i_{s2} the secondary windings consist of massive copper conductors that represent 1 winding turn and can be also equipped with adequate cooling channels [3,6]. In the presented case the massive secondary turns were furthermore divided into two halves of individual cross sections $17 \text{ mm} \times 2 \text{ mm}$, where the total cross section of a secondary winding was $17 \text{ mm} \times 4 \text{ mm}$. In the presented case both the primary as well as the secondary windings consist of two parallel branches that are placed on the opposite parts of the core. The final assembly is furthermore mechanically reinforced as the transformer is exposed to high mechanical stress due to high currents in the windings [1]. The presented transformer is designed for operation at the frequency of 1 kHz.

2.2. Operation of the Welding Transformer inside the RSW System

The presented transformer is only a part of the RSW system. The transformer is on the primary side connected to the H-bridge and on the secondary side to the output rectifier, as shown in Figure 1. Both connected parts determine the operation of the transformer, that is, how the electromagnetic variables inside the discussed transformer change with time. These variables generate power loss inside the transformer, therefore the analysis of operation is crucial. The operation of the RSW system can be broken down into 4 characteristic states that depend on the state of the H-bridge converter. These 4 states are shown in Figure 3.

In the presented case, T_p represents the time of one modulation period, T_{ON} is the time period in which relevant transistors are set in such a way that the transformer is supplied from the DC-link and T_{OFF} is the time period when all the transistors are not conducting and thus separate the transformer from the DC-link voltage. The typical 4 operation states hence correspond to conduction states of

switches S_1 , S_2 , S_3 and S_4 of the H-bridge converter, which supplies the primary winding of the transformer either with voltage $u_p = U_{dc}$, $u_p = 0$ or $u_p = -U_{dc}$. The primary current i_p corresponds to the waveform of the generated voltage u_p , where the current increases or decreases according to the individual switching state. Each conducting switching state (states 1 and 3 in Figure 3) is followed by a short additional state (states 2a and 4a), where absolute value of i_p continuously decreases to 0 despite all transistors are already turned off. In these states the current i_p flows through the free-wheeling diodes of the H-bridge. However, the impact on power loss of these states is in this paper neglected due to a very short duration of these two states.

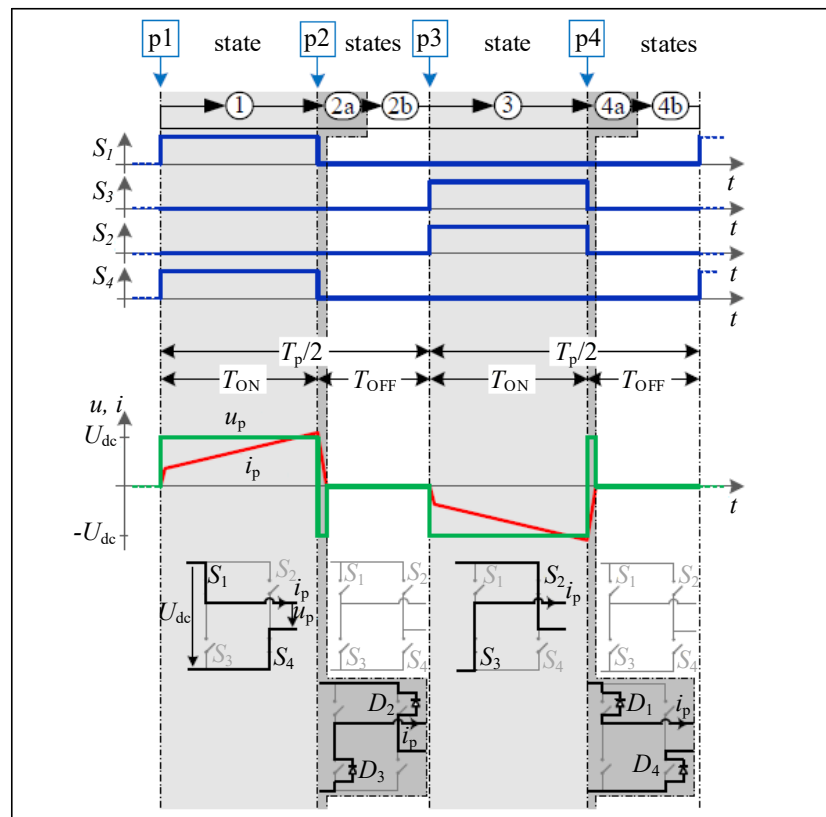


Figure 3. Pulse-width modulation with corresponding current and voltage on the primary side of the resistance spot welding (RSW) transformer [8].

The presented states in the primary winding generate also 4 main states in the secondary winding. These states depend on the output rectifier and are shown in Figure 4.

On the secondary side of the transformer the currents i_{s1} and i_{s2} flow only when individual rectifier diodes are polarized in a conducting way. Due to the inductive nature of the load, the presented converter operates in the continuous conducting mode on the secondary side of the transformer, that is, the current i_1 flows also in states 2 and 4, where it splits equally through the two secondary windings [4,6]. Analogous to the primary side, there are also two brief switching states 2a and 4a that are in the presented analysis omitted. The generated continuous DC welding current i_1 is finally used to generate welds of adequate quality.

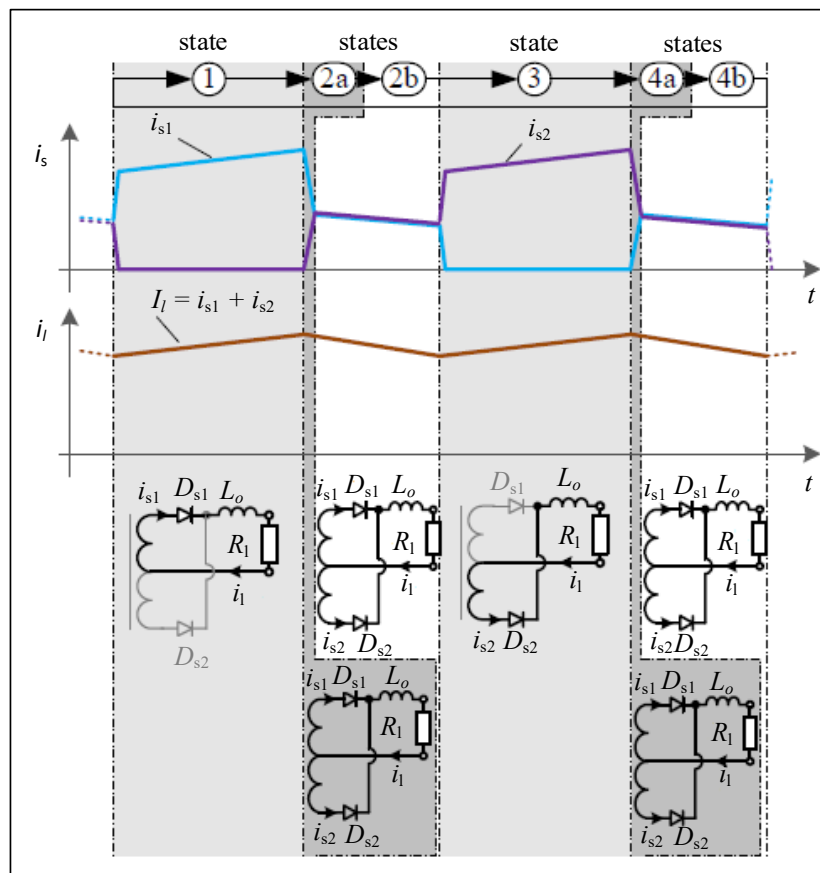


Figure 4. Typical states of the secondary side of the RSW transformer and output rectifier [8].

2.3. Power Loss Inside the Welding Transformer

Power loss inside the welding transformer can be in general separated in the iron core and winding power loss components. Both components are heavily dependent on used materials, design as well as the operation of the transformer [3,7].

The operation of the RSW system is for the needs of the presented analysis divided into 4 characteristic states as discussed in previous subsection. These 4 states can be furthermore combined into 3 characteristic conduction states of the transformer:

- State 1: The electrical current flows through the secondary winding 1 and the primary winding,
- State 3: The electrical current flows through the secondary winding 2 and the primary winding,
- State 2b and 4b: The electrical current flows only through the secondary windings.

These three states are determined by the direction of the currents and the activity of the windings in the transformer as shown in Figure 5.

In each of the presented state the excitation of the magnetic subsystem is substantially different; the currents in individual windings generate magneto-motive force (mmf) Θ along the iron core, which furthermore generates the magnetic flux and linkage between primary and secondary windings. The generated magnetic flux is, however, flowing not only in the magnetic core. Due to imperfections of the used materials (permeability of the iron core is not infinite, permeabilities of copper and air are not zero), magnetic flux is generated also in the areas around the core. Such areas include all the areas where mmf is generated, that is, areas where windings are located.

Due to the specific design, mmf in the iron core window acts predominantly along the y -direction. According to the presented conduction states, the distribution of the mmf $\Theta_y(x)$ in the iron core

window can be easily approximated by considering that the density of current in the windings is uniform. According to the Ampere’s Law, Θ_y is therefore changing linearly in respect to the length of the core window (x -axis) as shown in Figure 6a).

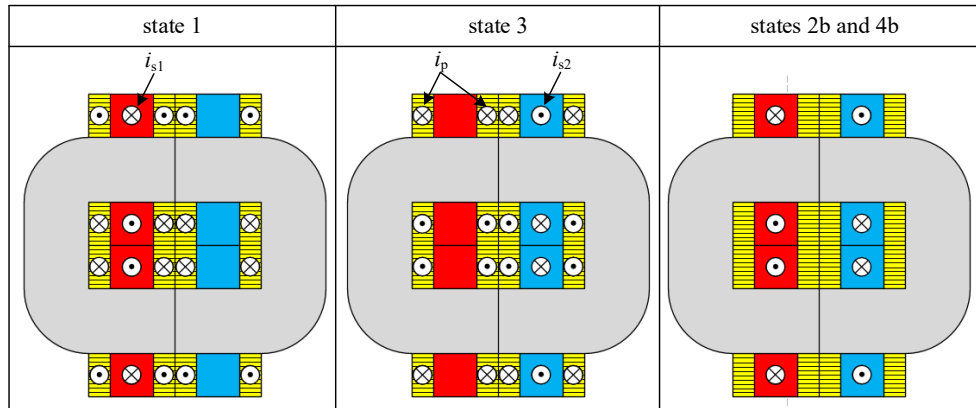


Figure 5. Current direction and winding activity for all four characteristic switching states of the RSW system [8].

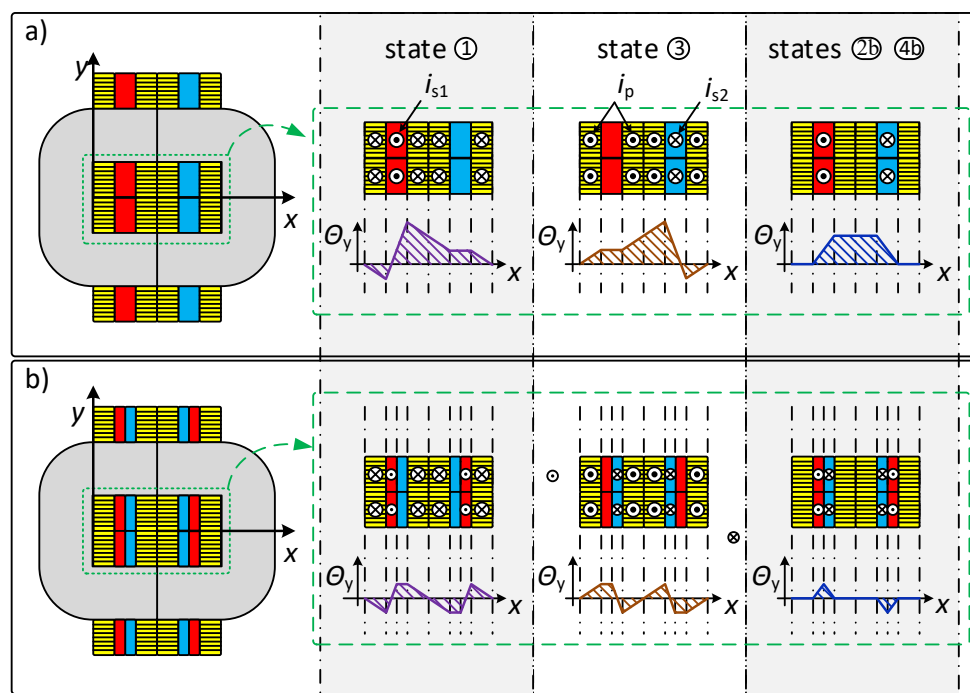


Figure 6. Two types of distribution of windings and a comparison of magneto-motive force for all states: (a) distribution of winding layout 1 and (b) distribution of winding layout 2 [8].

The obtained results have shown that the mmf distribution $\Theta_y(x)$ in different conducting states changes significantly. As the magnetic flux Φ_y is a direct consequence of $\Theta_y(x)$ and in the transformer window only linear magnetic materials (copper, air, insulation) are used, the distribution of the flux $\Phi_y(x)$ in this area corresponds to the $\Theta_y(x)$. The significant changes in $\Theta_y(x)$ consequently generate significant changes in $\Phi_y(x)$. As this leakage flux is changing mostly in electrically conducting

materials (windings and iron core), the corresponding induced voltage generates unwanted eddy currents that increase the power loss in the device.

By analyzing the original winding layout shown in Figure 6a it was shown that the distribution of mmfs in individual conduction states is very imbalanced with relative high peak values. Moreover, the change of distribution $\Theta_y(x)$ between the states is significant. The generated mmf is acting in the y -direction, hence also the corresponding leakage flux will flow across the transformer window in this direction. This leakage flux changes significantly with time and induces voltages in the conducting materials of the transformer. The discussed induced voltage in the windings is causing the so called proximity effect, whereas the induced voltage in the iron core is causing additional eddy currents. Both effects are qualified as so called dynamic power loss, because they are generated due to changes of electromagnetic variables. These loss components increase the total loss significantly and should therefore be minimized. The imbalanced leakage magnetic field distribution $\Phi_y(x)$ furthermore leads to imbalanced flux in the iron core and can cause local iron core saturation in addition to increased power loss. This can again lead to increased power loss of the device, as the magnetizing current in the primary windings increases, which can be visible as characteristic current spikes in the primary current [6,9].

The key for discussed loss reduction was clear; the winding layout of the transformer should be designed in such a way that the distribution of the produced mmfs $\Theta_y(x)$ is in all conduction states balanced, whereas the peak values of Θ_y along the x axis should be held as low as possible. This can be achieved, for example, using the winding arrangement shown in Figure 6b. In comparison to original winding layout shown in Figure 6a, in this case the secondary windings are divided in two parallel branches that balance the mmf distribution in all states. Importantly also the peak values in $\Theta_y(x)$ are reduced for more than 50 %, therefore the changes between the distributions in individual conducting states are significantly smaller. In this way the dynamic loss components of the transformer were significantly reduced what was confirmed with the experimental analysis presented in following subsections.

3. Laboratory Experimental System

The presented simplified theoretical analysis was applied due to the very complex nature of the problem. In a real transformer, $\Theta_y(x)$ is due to possible skin and proximity effects not changing necessarily linearly in respect to x -axis. Consequently also $\Phi_y(x)$ in the core window can be distorted (however still imbalanced in a similar fashion as in the discussed linear analysis). Furthermore, the windings outside of the transformer core produce mmf that cannot be approximated using only the component in the y -axis. Lastly, the connections between the transformer and output rectifier should be considered as they impact the operation of the whole system significantly. Due to these facts simulation analysis would require very complex models (e.g., a 3D finite element model) where the theoretical background of the increased additional loss components could be overlooked. Such models furthermore cannot include all the effects, especially the increased eddy currents in the iron core that occur due to leakage magnetic fields that are perpendicular to core lamination. Consequently the analysis was carried out using a laboratory experimental systems that is presented below.

The laboratory experimental system was designed in such a way that changes of various winding arrangements could be performed. For this purpose a typical industrial RSW transformer was adjusted with additional bus system on the secondary side of the transformer, as shown in Figure 7. This system consisted of three buses; upper and lower buses (marked by 1 and 3 in Figure 7) were connected to both diodes of output rectifier, whereas the middle bus (marked by 2 in Figure 7) represents the center tap of the transformer and therefore the negative potential of the full wave rectifier.

The presented buses were designed in such a way that changing of the position of secondary and primary windings was possible. In order to enable the discussed analysis, also secondary windings of the transformer were adjusted. In a typical industrial RSW transformer, both secondary windings consist of single massive copper conductors that are equipped with cooling channels. In contrast to

this, the secondary windings of the laboratory transformer were split into two halves as shown in Figure 2, where the cooling channels were omitted. In this way, comparable results for the presented analysis were obtained.

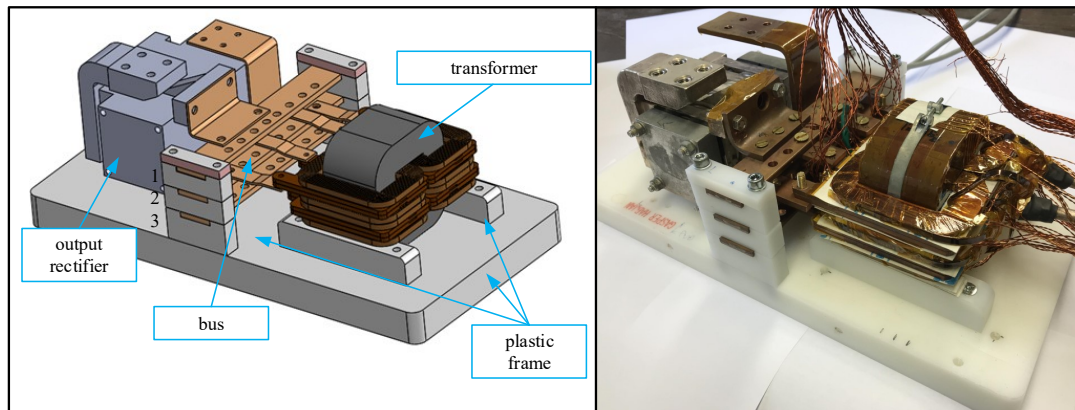


Figure 7. Design of the laboratory experimental system [1].

The drawback of the additional bus system was, however, that the total resistances on the secondary side of the transformer were increased in comparison to a compact industrial RSW transformer [5]. The measured total resistances for both winding arrangements are shown in Table 1. Measurements of resistances were performed using an adequate bridge based DC micro ohm meter which measured a DC resistance.

Table 1. Total resistance of individual windings for both winding arrangements.

	Primary Winding	Secondary Winding 1	Secondary Winding 2
distribution of winding layout 1	$R_p = 23.7 \text{ m}\Omega$	$R_{s1} = 0.137 \text{ m}\Omega$	$R_{s2} = 0.184 \text{ m}\Omega$
distribution of winding layout 2	$R_p = 23.7 \text{ m}\Omega$	$R_{s1} = 0.106 \text{ m}\Omega$	$R_{s2} = 0.111 \text{ m}\Omega$

From the obtained measurements it was shown that the total secondary resistance (windings combined with the bus system) was lower for proposed winding arrangement in comparison to the original arrangement. This was due to slightly shorter net path of the currents through the winding combined with the connection between the transformer and the output rectifier. Furthermore, the total resistances of both secondary branches were better balanced compared to the original arrangement. An imbalance of secondary resistance can lead to drift of magnetic flux inside the core and consequently to its saturation [6,8,9]. Furthermore, the iron core of the transformer was equipped with several measuring coils as shown in Figure 8.

These measurement coils were used to calculate the density of magnetic flux inside the core, where in each measurement coil induced voltage $u_i(t)$ was measured. The densities of magnetic flux $B(t)$ were obtained by (1)

$$B(t) = \frac{1}{N_m S} \int u_i(t) dt, \quad (1)$$

where S represents the cross-section of the core and N_m represents the number of turns of the measurement winding. The laboratory experimental system was finally mechanically reinforced using an adequate plastic frame.

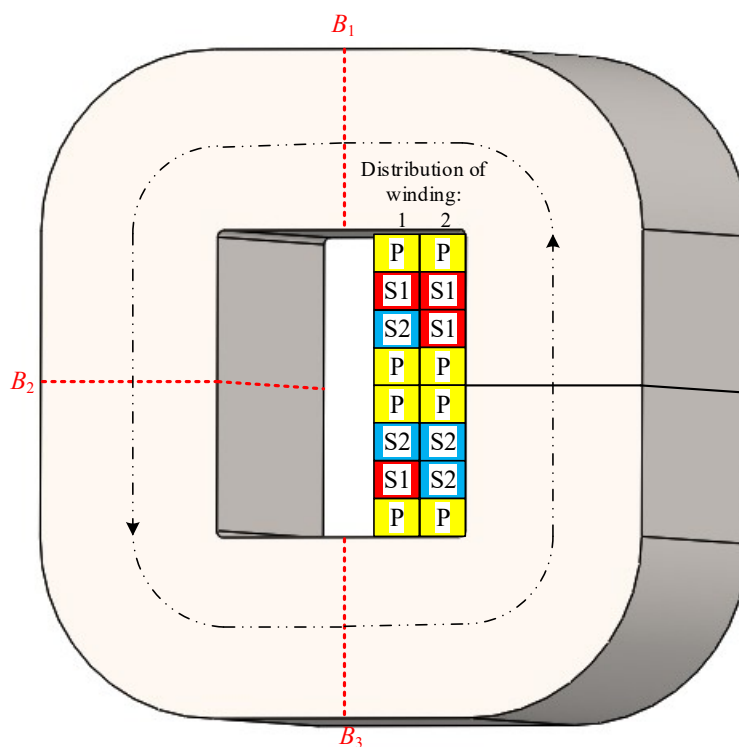


Figure 8. Placement of measuring coils on the core of laboratory RSW transformer [1].

4. Results

The discussed laboratory experimental system was tested for both winding arrangements using equal operation conditions. The tests were performed in such a way that the load resistance R_1 and inductance L_1 of the system were fixed, whereas the duty ratio of the H-bridge inverter was increased from 0.3 to 0.8 with a step of 0.1. The efficiency was determined by measuring the voltages and currents on the primary and secondary side of the transformer. Measurements were performed using the high performance measuring device DEWETRON DEWE-2600, where the voltages were measured directly and for the measurements of the currents special low frequency Rogowski's coils (CWT 3LFR and CWT 150LFR) were used.

Measured voltages for duty ratio of 0.6 are shown in Figure 9.

The obtained result have shown that the induced voltages in the secondary windings were slightly higher in the proposed winding arrangement in comparison to the original one. The RMS values of induced voltages in the secondary windings in the case of winding arrangement 1 were $U_{s1RMS} = 5.129$ V and $U_{s2RMS} = 5.225$ V. Compared to this, when winding arrangement 2 was applied, these values were $U_{s1RMS} = 5.249$ V and $U_{s2RMS} = 5.268$ V. This increase was attributed to lower leakage magnetic fields in the transformer window combined with lower total resistances on the secondary side of the transformer when improved winding arrangement was applied. Corresponding currents are shown in Figure 10.

The difference between all the currents in both analyzed winding arrangements was significant. The average steady state value of output welding current i_1 was in the presented operation point for 1780 A higher, what accounts for 12.7%. This increase was attributed to higher induced voltages in both secondary windings as well as lower total resistances on the secondary side of the RSW transformer.

Based on measured voltages $u(t)$ and currents $i(t)$ during the welding cycles, average input as well as output powers for different duty ratios were calculated. All the average power values P were determined using orthogonal decomposition technique in the time domain, where measured currents were decomposed into orthogonal and co-linear components in respect to adequate voltages [10,11]. In this way, from measured primary voltage u_p and current i_p the average input power of the

transformer P_{in} was calculated and from measured secondary voltages u_{s1} and u_{s2} as well as currents i_{s1} and i_{s2} average output powers of the transformers P_{out1} and P_{out2} were calculated, respectively. The total output average power was determined by $P_{out} = P_{out1} + P_{out2}$. Based on the obtained P_{in} and P_{out} , total power loss P_{tr} and efficiency η_{tr} of the transformer were calculated by (2) and (3), respectively.

$$P_{tr} = P_{in} - P_{out} \quad (2)$$

$$\eta_{tr} = \frac{P_{out}}{P_{in}} \quad (3)$$

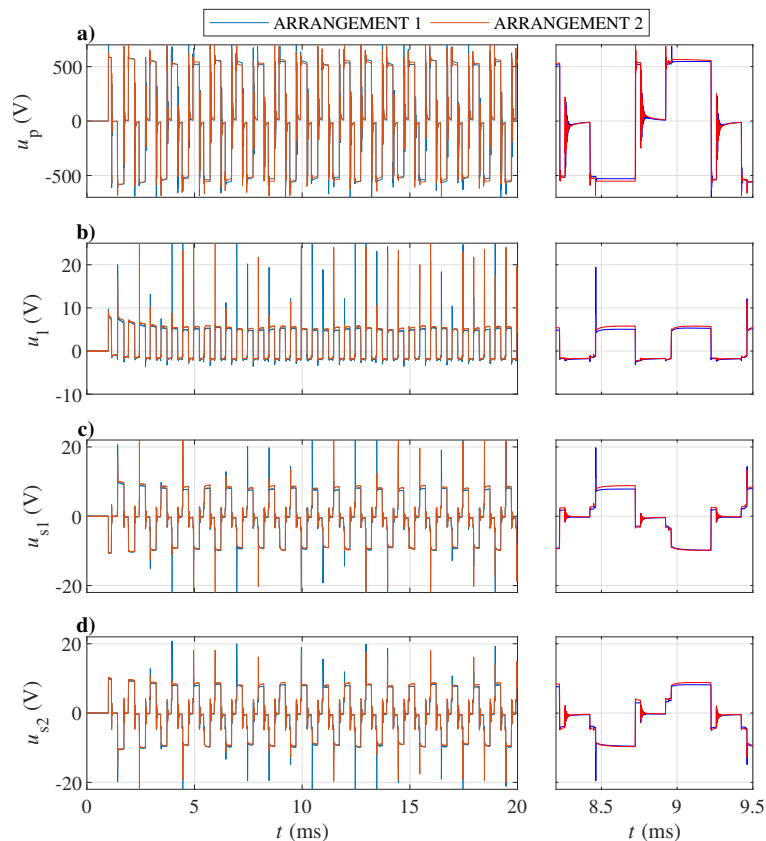


Figure 9. Comparison of measured primary and secondary voltages for both winding arrangements: (a) voltage in the primary winding u_p , (b) output voltage u_1 , (c) voltage in the secondary winding 1 u_{s1} and (d) voltage in the secondary winding 2 u_{s2} .

In addition to P_{tr} , also the total power loss of the output rectifier P_{rect} was determined. For this purpose furthermore the voltage u_1 and current i_1 on the output of the rectifier were measured. Based on these measurements, the average power supplied to the load P_{load} was determined. The power loss in the full-wave rectifier was obtained by (4)

$$P_{rect} = P_{out} - P_{load}, \quad (4)$$

whereas the efficiency of the output rectifier was calculated by (5) respectively.

$$\eta_{rect} = \frac{P_{load}}{P_{out}}. \quad (5)$$

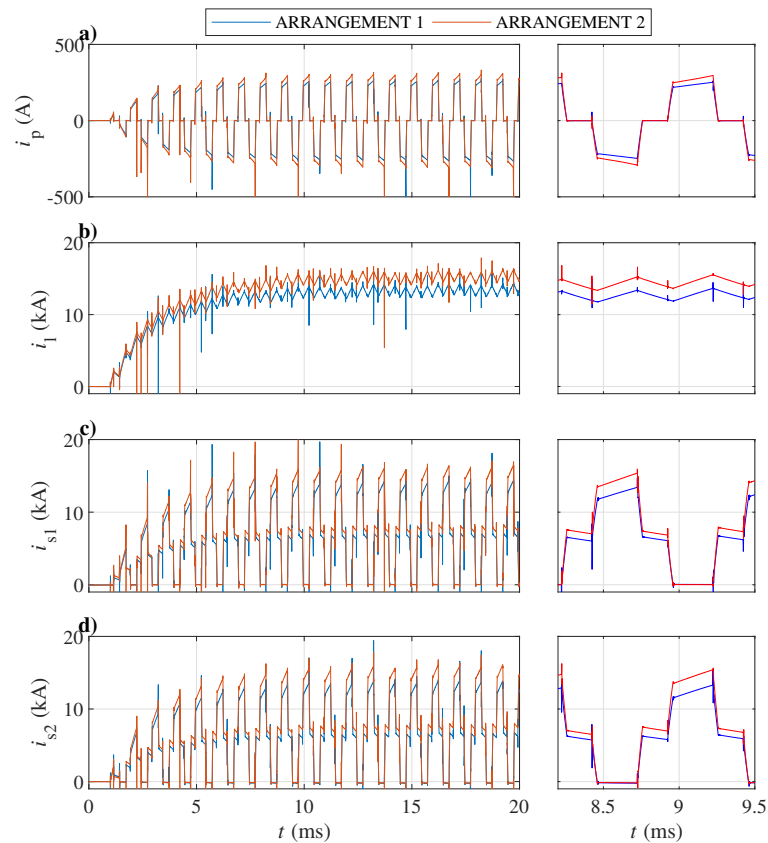


Figure 10. Comparison of measured primary and secondary currents for both winding arrangements: (a) current in the primary winding i_p , (b) welding current i_l , (c) current in the secondary winding 1 i_{s1} and (d) current in the secondary winding 2 i_{s2} .

Due to the difference in the output currents for both winding arrangements, the obtained results were compared in respect to the output current instead of the duty ratio. The obtained results are presented in Figure 11.

The obtained results have shown that the efficiency of the transformer with improved winding arrangement was significantly higher; the efficiency improved for around 5% at low and around 6.7% at high welding currents, where the average efficiency difference between both distributions of windings was 6.27%. This increase corresponded to around 0.73 kW or 6 kW less total power loss in the transformer at low and high welding currents, respectively. In this way P_{tr} was decreased for 31.7–34.7%. This decrease of power loss was a direct consequence of the decreased leakage magnetic field inside the transformer window and generates the additional dynamic power loss component. Due to improved winding arrangement the proximity effect between all the winding coils was significantly reduced. Furthermore, as the leakage magnetic flux entered the iron core perpendicular to the lamination of iron core, the dynamic loss inside the iron core was reduced also. Changes of magnetic flux that enters the iron core perpendicular to lamination generate eddy currents that are due to unfavorable direction not limited by the lamination. This effect can increase the iron core power loss significantly [12]. The decrease of P_{tr} consequently enables to reduce the cooling of the transformer what furthermore increases the efficiency of the whole RSW system. In this way also weight of the transformer can be reduced, whereas the power density is improved.

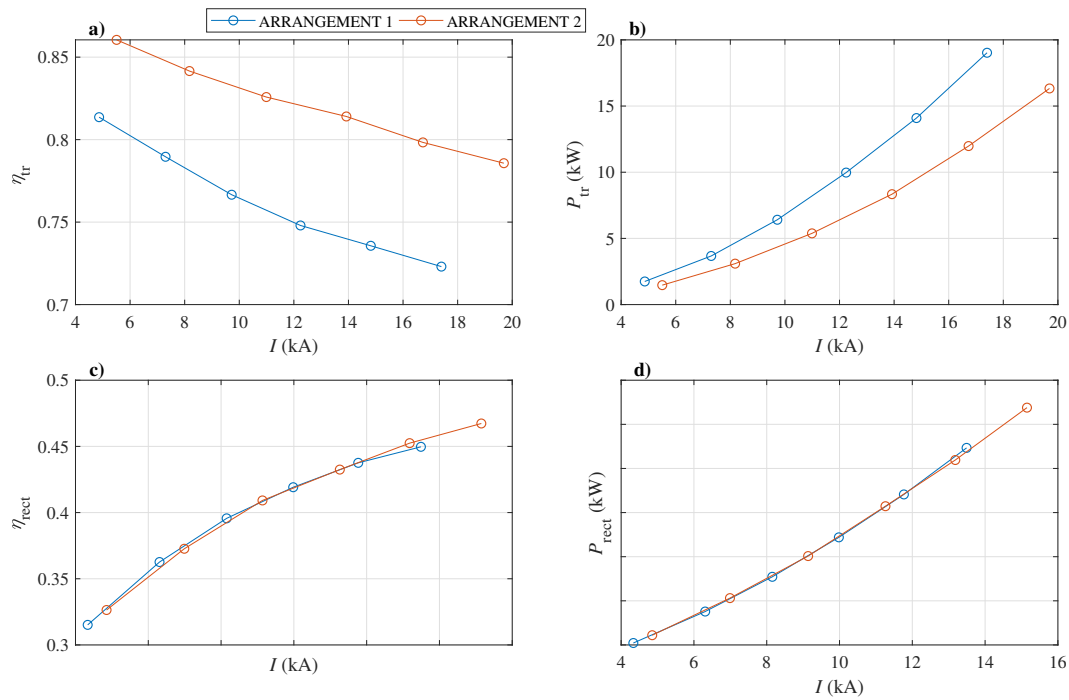


Figure 11. Comparison of determined power loss and efficiency of the transformer (a,b) and output rectifier (c,d) for both winding arrangements.

In contrast to the transformer, the efficiency and power loss of the rectifier depended only on the output current. Therefore the results were comparable for both winding arrangements. It is worthwhile to note that the rectifier power loss was even higher than power loss of the transformer.

Using the measurement coils on the core as presented in Figure 8 distribution of magnetic flux inside the iron core was determined. The obtained results are presented in Figure 12, where the imbalance of magnetic flux in the iron core was observed.

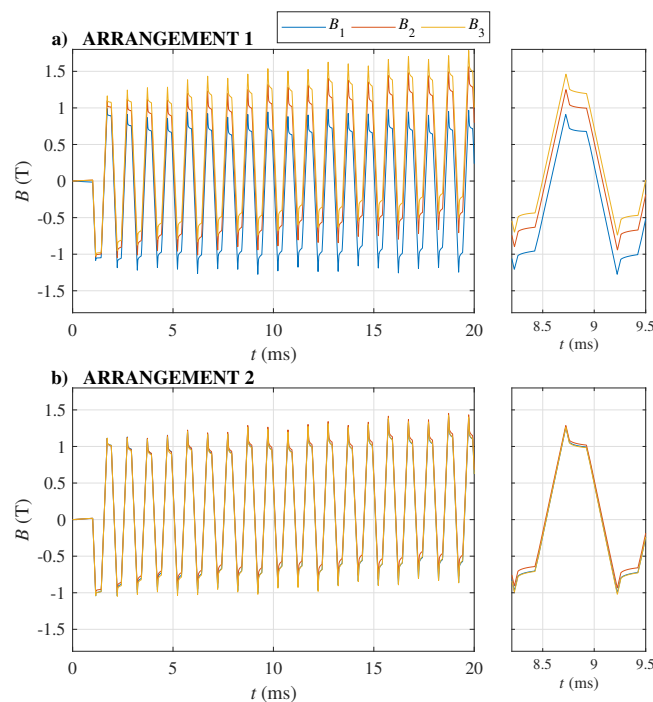


Figure 12. Results of the calculated densities of magnetic flux density B for: (a) arrangement 1 and (b) arrangement 2.

The calculated densities of magnetic flux were substantially different in all three core parts when original winding arrangement was analyzed (Figure 12a)). In contrast to this, all three densities of magnetic flux were balanced when the improved winding arrangement was analyzed. The observed non-uniform distribution of B was a direct consequence of imbalanced distribution $\Theta_y(x)$ through all 4 characteristic states. As $\Theta_y(x)$ was balanced in all the states if improved winding arrangement was applied, consequently also a uniform distribution of B inside the core was achieved. A non-uniform distribution of B can lead to local iron core saturation and consequently to increased power loss and decreased operation reliability of the device.

5. Conclusions

In the paper, the impact of winding arrangements on dynamic power loss inside a RSW transformer was analyzed. The layout of the windings along the transformer's core has direct impact on amplitudes and distribution of leakage magnetic fields around these windings. First a sound theoretical background for improvement of winding arrangements is discussed, where the negative consequences of discussed phenomena were pointed out. The negative consequences include increased dynamic power loss inside the windings (proximity effect) and the iron core (increased eddy currents) as well as non-uniform distribution of magnetic flux density inside the core, which can lead to local saturation. The theoretical analysis was confirmed by experimental results. The obtained experimental results have shown that the losses inside the transformer were significantly decreased when the arrangement of the windings was improved with accordance with the presented theoretical background. The efficiency of the improved transformer was in average increased for 6.27 %. With the experimental analysis it was furthermore shown that the improved winding arrangement results in a better distribution of magnetic flux density inside the core. Consequently, local saturations of the core were avoided, whereas the magnetic material inside the device was better utilized. The presented analysis therefore points out basic guidelines when designing a high power DC-DC converter that utilizes a transformer with a center tapped rectifier. Future work will be focused on analysis of the non-uniform distribution of the magnetic field on the operation and losses of the whole system for RSW.

Author Contributions: Supervision, M.P.; Writing—original draft, G.H. and M.P.; Writing—review & editing, M.P.

Funding: This research received no external funding.

Conflicts of Interest: The authors declare no conflict of interest.

Abbreviations

The following abbreviations are used in this manuscript:

RSW	Resistance Spot Welding
DC	Direct Current
AC	Alternating Current
PWM	Pulse Width Modulation
mmf	magneto-motive force

References

1. Habjan, G. Nonhomogeneous Distribution of Magnetic Flux inside the core of a Resistance Spot Welding Transformer. Master's Thesis, Faculty of Electrical Engineering and Computer Science, University of Maribor, Maribor, Slovenia, 2018.
2. Kimchi, M.; Phillips, D.H. *Resistance Spot Welding: Fundamentals and Applications for the Automotive Industry*; Morgan & Claypool: San Rafael, USA, 2017; p. i-115
3. Popović Cukovic, J. Development of Winding design for Resistance Spot Welding Transformer. Ph.D. Thesis, Faculty of Electrical Engineering and Computer Science, University of Maribor, Maribor, Slovenia, 2013.
4. Zhou, K.; Yao, P. Review of Application of the Electrical Structure in Resistance Spot Welding. *IEEE Access* **2017**, *5*, 25741–25749. [[CrossRef](#)]

5. Brezovnik, R.; Černelič, J.; Petrun, M.; Dolinar, D.; Ritonja, J. Impact of the Switching Frequency on the Welding Current of a Spot-Welding System. *IEEE Trans. Ind. Electron.* **2017**, *64*, 9291–9301. [[CrossRef](#)]
6. Klopčič, B.; Dolinar, D.; Štumberger, G. Advanced Control of a Resistance Spot Welding System. *IEEE Trans. Power Electron.* **2008**, *23*, 144–152. [[CrossRef](#)]
7. Podlogar, V.; Klopčič, B.; Stumberger, G.; Dolinar, D. Magnetic Core Model of a Midfrequency Resistance Spot Welding Transformer. *IEEE Trans. Magn.* **2010**, *46*, 602–605. [[CrossRef](#)]
8. Petrun, M. Modeling and Analysis of Magnetic Components in High Power DC-DC Converters. Ph.D. Thesis, Faculty of Electrical Engineering and Computer Science, University of Maribor, Maribor, Slovenia, 2014.
9. Štumberger, G.; Klopčič, B.; Deželak, K.; Dolinar, D. Prevention of Iron Core Saturation in Multi-Winding Transformers for DC-DC Converters. *IEEE Trans. Magn.* **2010**, *46*, 582–585. [[CrossRef](#)]
10. Štumberger, G.; Polajžer, B.; Toman, M.; Dolinar, D. Orthogonal decomposition of currents, power definitions and energy transmission in three-phase systems treated in the time domain. In Proceedings of the International Conference on Renewable Energies and Power Quality (ICREPQ'06), Palma de Mallorca, Spain, 5–7 April 2006; Volume 1, pp. 263–267. [[CrossRef](#)]
11. Williams, J.L. A New Interpretation of the Akagi-Nabae Power Components for Nonsinusoidal Three-Phase Situations. *IEEE Trans. Instrum. Meas.* **1992**, *4*, 523–527. [[CrossRef](#)]
12. Cougo, B.; Tüysüz, A.; Mühlethaler, J.; Kolar, J.W. Increase of tape wound core losses due to interlamination short circuits and orthogonal flux components. In Proceedings of the IECON 2011—37th Annual Conference on IEEE Industrial Electronics Society, Melbourne, VIC, Australia, 7–10 November 2011; pp. 1372–1377.



© 2019 by the authors. Licensee MDPI, Basel, Switzerland. This article is an open access article distributed under the terms and conditions of the Creative Commons Attribution (CC BY) license (<http://creativecommons.org/licenses/by/4.0/>).